Supporting Information

Polarization-Induced Nanohelixes of Organic Cocrystals from Asymmetric Component and Chirality Inversion

Jinqiu Chen, [a] Canglei Yang, [a] Shuang Ma, [a] Zhiqi Liu, [a] Wenxin Xiang, [a] Jing Zhang *[a]

***Jing Zhang** - State Key Laboratory of Organic Electronics and Information Displays & Institute of Advanced Materials (IAM), Nanjing University of Posts & Telecommunications, 9 Wenyuan Road, Nanjing 210023, China;
E-mail: iamjingzhang@njupt.edu.cn.

Table of Contents

Experimental Procedures

Materials. DBCz and DNF were purchased from Aladdin Corp, TCNQ and DTTCNQ were purchased from Luminescence Technology Corp, TCAF was purchased from Sigma-Aldrich. All of them were used directly as received without further purification. All solvents were HPLC grade.

Polymorphic Crystals Growth and Structural Analysis. DBCz-TCNQ complexes were prepared by chloroform solution. First, dissolve the mixture of DBCz and TCNQ (molar ratio of 1:1) in chloroform to obtain a solution with a concentration of 1.8 mg/mL. After heating at 70 °C for 1 hour to ensure complete dissolution, the mixed solution was left in the air to slowly evaporate for three to four days, until the liquid completely disappeared and black needle-like crystals were finally found at the bottom of the bottle. Subsequently, the needle cocrystals were washed from the vial with petroleum ether and dried in the air. For DNF-TCAF cocrystals, they were prepared by chlorobenzene solution. First, dissolve the mixture of DNF and TCAF (molar ratio of 1:1) in chlorobenzene to obtain a solution with a concentration of 1.8 mg/mL. After heating at 70 °C for 1 hour to ensure complete dissolution, the mixed solution was then left in the air to slowly evaporate for three to four days, black needle-like crystals would be found at the bottom of the bottle. The Bruker smart-1000-CCD diffractometer with graphite-monochromatic Mo *K*α radiation (λ = 0.71073 Å) was used to measure the crystal structures of single crystals. X-ray crystallography data was collected at room temperature. The structure was resolved by the direct method and refined by the full-matrix least-squares method on F^2 using the SHELXL-97 program.

Growth of the Micro/nanocrystals on the Substrates. In order to grow micro/nano crystals on the substrate, an acetonitrile solution (1.8 mg/mL) containing DBCz and TCNQ in a molar ratio of 1:1 was drop-casted onto the SiO_2/Si substrate; an chlorobenzene solution (1.8 mg/mL) containing DNF and TCAF in a molar ratio of 1:1 was drop-casted onto the SiO_2/Si substrate. As the solvent evaporating, belt-shaped crystal was prepared on the substrate.

Measurements. The nanostructures of the complex were characterized by optical microscopy (BX53, Olympus), UV–visible absorption spectrum (LAMBDA 35), circular dichroism spectrum (JASCO, J-815), Atomic force microscopy (Bruker Dimension Icon), Scanning electron microscope (Bruker, S4800), Transmission electronic microscopy (HITACHI HT7700) and corresponding selected-area electron diffraction (HITACHI HT7700). PXRD was measured on a D/max2500 with Cu *K*α source (κ = 1.541 Å).

The elastic energy of nanocrystals. The corresponding elastic energy of the helical nanobelts:

$$\Delta E_{elastic} \approx \frac{\pi WY}{24R} t^3 \qquad ①$$

$$\Delta E \approx \Delta E_{electro} + \Delta E_{elastic} \qquad ②$$

The R value is approximately taken as $W/2$. Equation ① is the elastic energy, and Y is the banding modulus. In order to maintain the helical morphology of the crystal, the elastic energy should be smaller than that of electrostatic energy, so that the total energy ΔE calculated by Equation ② is less than 0. A large σ will induce a large-scale twisting structure.

Results and Discussion

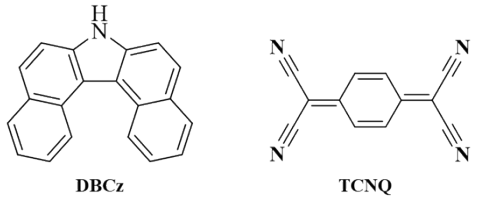

Figure S1. Molecular structure of DBCz and TCNQ.

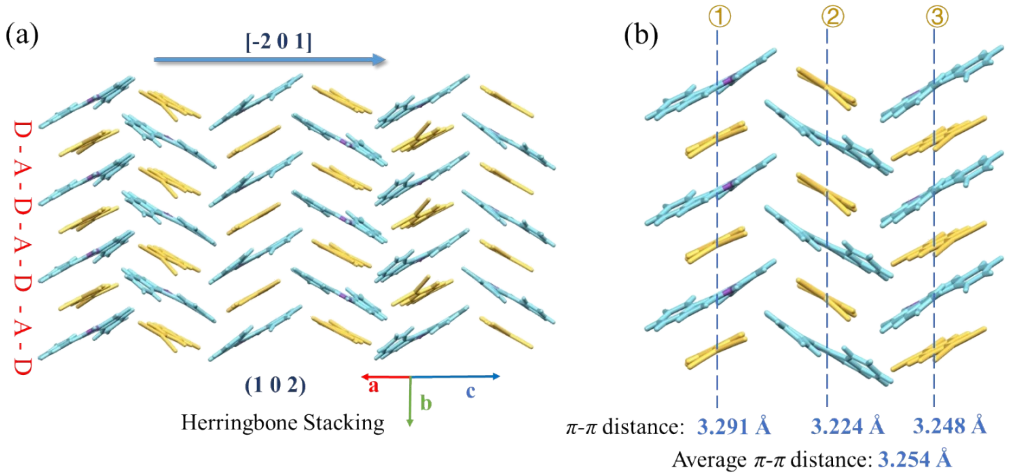

Figure S2. (a) Molecular packing pattern viewing along (102) face and (b) π-π distances in different stacked columns.

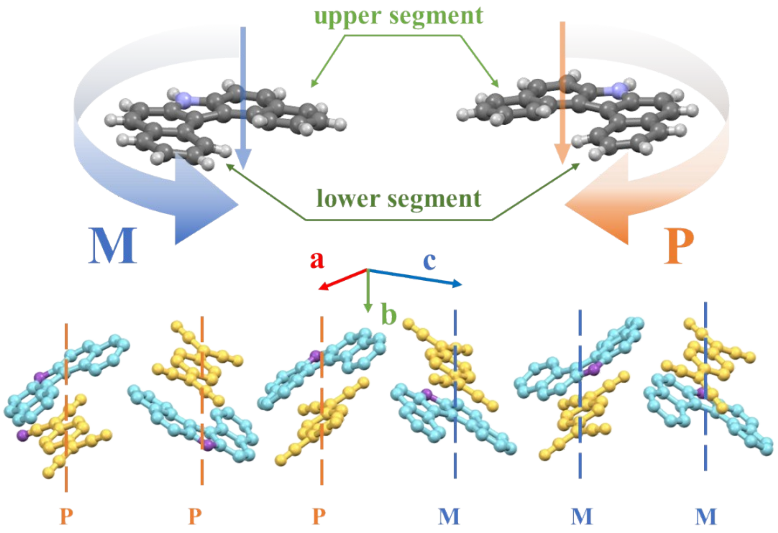

Figure S3. Alternate packing of DBCz molecules with P and M conformation.

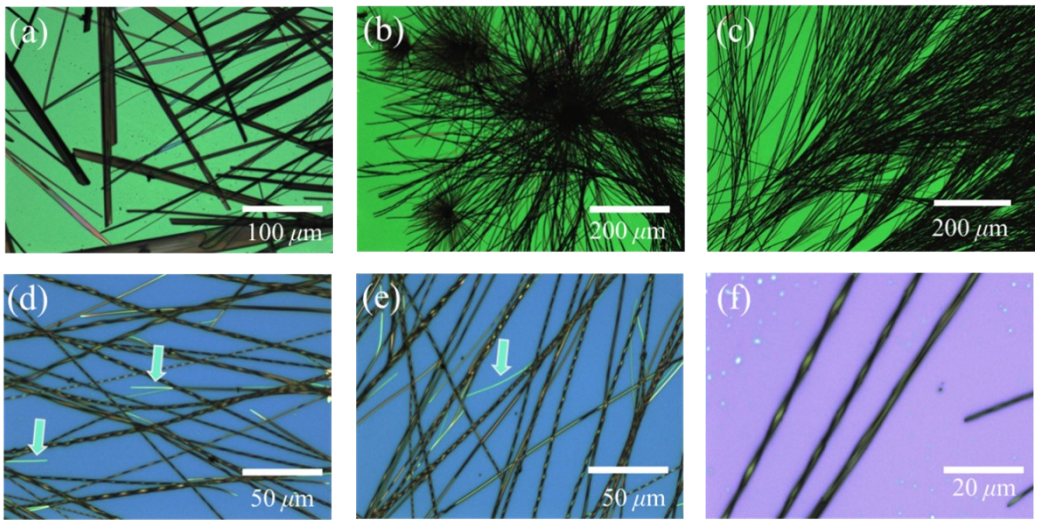

Figure S4. OM images of needle-shaped cocrystals and helical nanoribbons. Inside thin crystals at the green arrow were attached to the substrate.

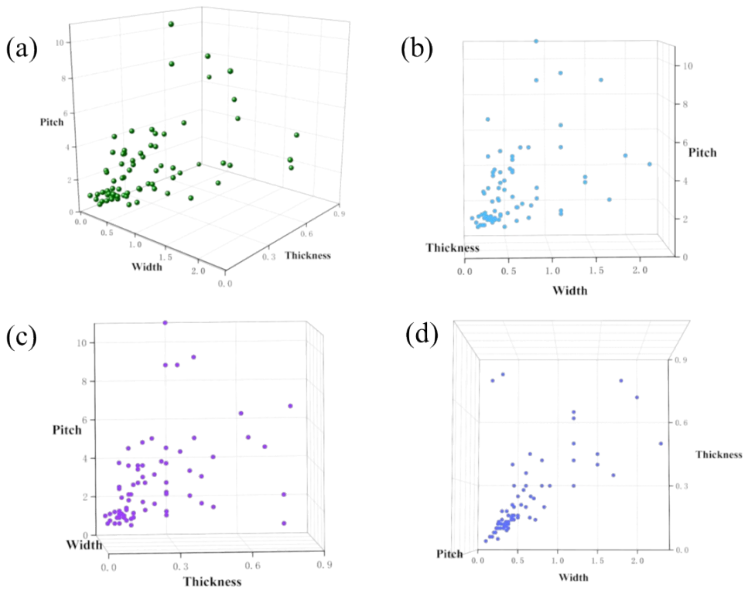

Figure S5. Width, thickness and pitch distributions of helical nanoribbons.

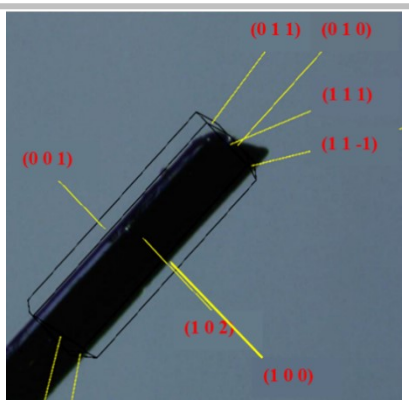

Figure S6. The crystal plane indication diagram of the crystal obtained by single crystal XRD.

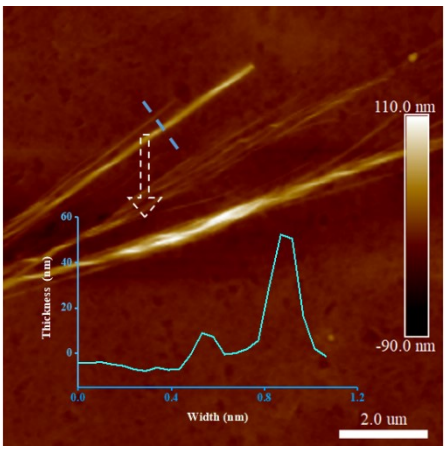

Figure S7. AFM image of helical crystals obtained by drop casting of the chloroform solution of DPP polymer and DBCz-TCNQ complex (5:95 mass ratio) on the substrate.

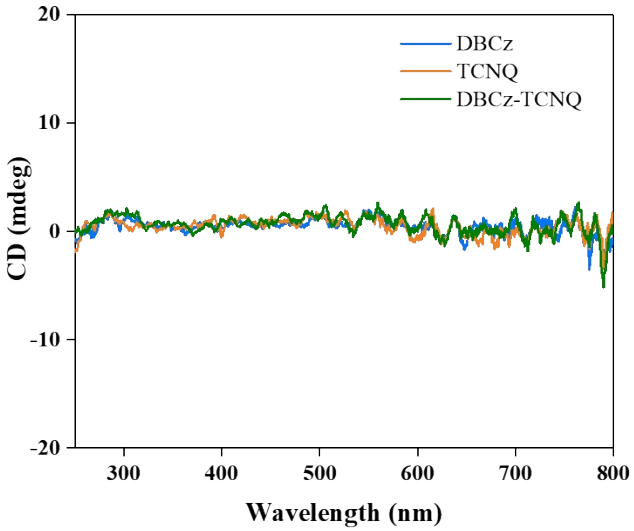

Figure S8. CD spectra of DBCz, TCNQ and DBCz-TCNQ solution.

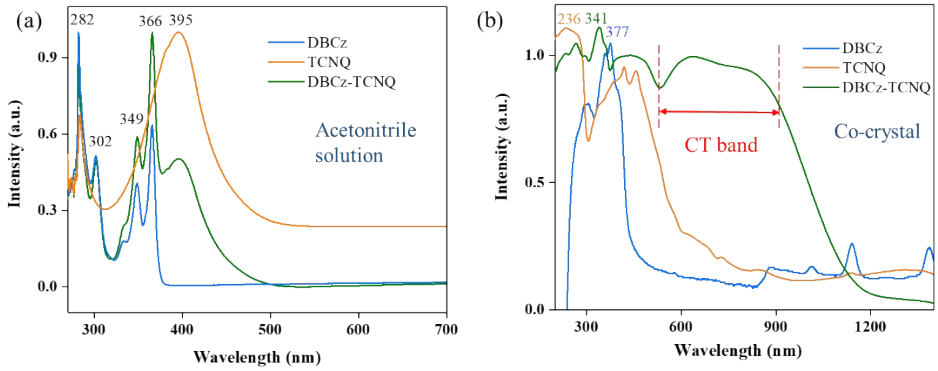

Figure S9. (a) UV-Vis absorption spectra of DBCz, TCNQ and DBCz-TCNQ solutions and (b) solid-state UV-Vis absorption spectra of DBCz, TCNQ powder and DBCz-TCNQ crystals.

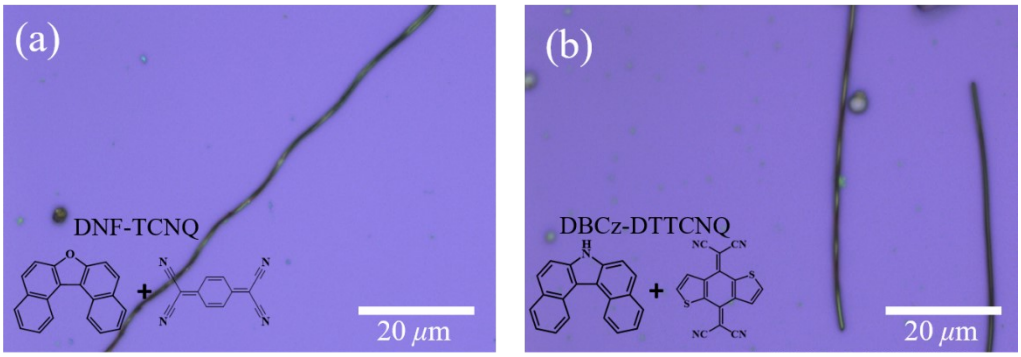

Figure S10. OM images of helical (a) DNF-TCNQ and (b) DBCz-DTTCNQ nanobelts on the substrates.

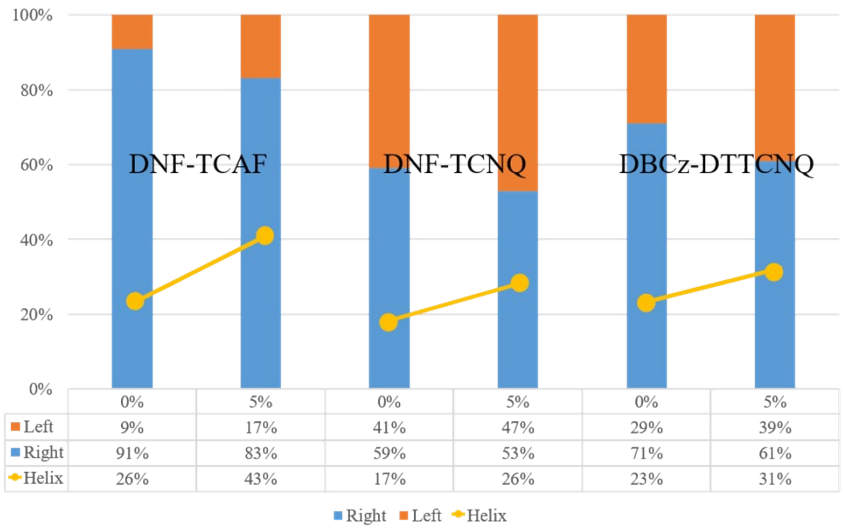

	0%	5%	0%	5%	0%	5%
Left	9%	17%	41%	47%	29%	39%
Right	91%	83%	59%	53%	71%	61%
Helix	26%	43%	17%	26%	23%	31%

Figure S11. Detailed morphological changes of DNF-TCAF, DNF-TCNQ and DBCz-DTTCNQ supramolecular constructs from blend solution with varying equivalents of BCz addition.

Table S1. Crystal data and structure refinements for DBCz-TCNQ and DNF-TCAF cocrystals.

	DBCz-TCNQ	DNF-TCAF
Formula	$C_{32}H_{17}N_5$	$C_{36}H_{16}N_6O$
Formula weight	471.50	548.55
Temperature (K)	150	296
Wavelength (Å)	1.542	1.367
Crystal system	Monoclinic	Triclinic
space group	*P*c	*P*1
Unit cell dimensions		
a (Å)	11.1150(6)	7.023(10)
b (Å)	7.4032(5)	9.909(14)
c (Å)	41.998(3)	11.109(14)
α (°)	90	65.89(6)
β (°)	93.750(5)	74.66(5)
γ (°)	90	73.28(4)
Volume (Å^3)	3448.5(4)	666.3(16)
Z	6	1
Absorption coefficient (mm^{-1})	0.653	0.086
F(000)	1464.0	282.0
Crystal size (mm)	0.13 × 0.11 × 0.1	0.12 × 0.11 × 0.1
θ range (°)	7.972 to 140.090	6.144 to 56.626
Limiting indices	$-13 \le h \le 13$	$-9 \le h \le 9$
	$-8 \le k \le 8$	$-11 \le k \le 13$
	$-50 \le l \le 51$	$-10 \le l \le 14$
Reflections collected	22382	5431
R(int)	0.0865	0.0240
Absorption correction	Semi-empirical from equivalents	Semi-empirical from equivalents
Refinement method	Full-matrix least-squares on F^2	Full-matrix least-squares on F^2
Data / restraints / parameters	11241/3/1008	3940/71/388
R [*I* > 2sigma(*I*)]	$R_1 = 0.0684$	$R_1 = 0.0842$
	w$R_2 = 0.1663$	w$R_2 = 0.1921$
R (all data)	$R_1 = 0.0980$	$R_1 = 0.1123$
	w$R_2 = 0.1892$	w$R_2 = 0.2096$
CCDC NO.	2169110	2214872

Table S2. The surface energy of different crystal faces.

hkl	Surface Energy (kcal/mol)
{102}	55.925
{100}	79.967
{002}	101.354
{-102}	132.433
{110}	167.719
{013}	168.702
{011}	169.612
{010}	173.799

Table S3. The attachment energy of different crystal faces in cocrystal.

hkl	Attachment Energy (kcal/mol)
{002}	-33.360
{102}	-40.359
{100}	-49.679
{10-2}	-90.360
{011}	-158.714
{010}	160.170